Adsorption of Phenol, Chlorophenols, and Dihydroxybenzenes onto Unfunctionalized Polymeric Resins at Temperatures from 294.15 K to 318.15 K

Katrin Wagner* and Siegfried Schulz

Universität Dortmund, Lehrstuhl für Thermodynamik, 44221 Dortmund, Germany

The surface excess for the adsorption of phenol, 2-chlorophenol, 4-chlorophenol, 2,4-dichlorophenol, 2,6-dichlorophenol, 2,4,6-trichlorophenol, 1,2-dihydroxybenzene, and 1,3-dihydroxybenzene from aqueous solution onto unfunctionalized polystyrene and polymethacrylate resins cross-linked with divinylbenzene (Lewatit VP-OC 1163, Amberlite XAD-4, Serdolite PAD I, II, and III, and Supelcogel TPR-100, respectively) at temperatures from 294.15 K to 318.15 K has been determined using the chromatographic method of frontal analysis. For a prediction of adsorption equilibria for phenol + water systems onto polymeric adsorbents, the fluid phase concentration is normalized to the solubility of the phenols in water. Isotherms of the Redlich−Peterson type with characteristic parameters for different polymers were fitted to the adsorption data (surface excess versus normalized concentration). The experimental data were correlated with a standard deviation of 1.1%; adsorption equilibria were predicted within 2%.

Introduction

Phenol is considerably important as a starting material for numerous intermediates and finished products in the chemical industry. It is used for the production of a wide range of consumer goods and process materials, for example, adhesives, impregnating resins, emulsifiers and detergents, plasticizers, herbicides, dyes, flavors, and additives for rubber chemicals.[1] The worldwide production of phenol is estimated to be 5 million tons per year.[2] Phenol is used in the production of phenol−formaldehyde resins, caprolactam, and bisphenol A, which is an important starting material for polycarbonates and epoxy resins.[3] Major sources of environmental contamination by chlorophenols are the widespread use of pentachlorophenol as a wood preservative, degradation products of chlorinated herbicides, the chlorination of lignin or the use of slimicides in paper or pulp mill plants, and the chlorination of municipal and industrial wastewater and drinking water.[4]

Due to the toxicity of phenols, their removal from water is an important issue. Different water treatment technologies are used to remove phenolic pollutants, for example, biological degradation, chemical oxidation, or adsorption. Adsorption processes can be used for a wide range of phenol concentrations and are cost-efficient, especially if the pollutants are to be recycled. In this context, polymeric adsorbents have gained in importance. Compared to the traditionally used active carbon, a smaller amount of adsorbent is required, longer residence times can be achieved, and the polymeric material can easily be regenerated.

For a broader industrial application of fluid phase adsorption, the availability of experimental adsorption data must be increased. Moreover, reliable models to predict adsorption equilibria are needed. In this paper, data for the adsorption of phenols from aqueous solution onto polymeric adsorbents are presented for various temperatures. The experimental data are correlated, and the possibility of predicting adsorption data is discussed.

* To whom correspondence should be addressed. E-mail: wagner@th.chemietechnik.uni-dortmund.de. Fax: +49 (0)231 755 2572.

Experimental Section

The adsorption systems examined in this work, that is, adsorbent (1) + adsorbate (2) + solvent (3), are listed in Table 1.

Materials. The following polystyrenes cross-linked with divinylbenzene were used as polymeric adsorbents: Lewatit VP-OC 1163 (Bayer AG, Leverkusen, Germany), Amberlite XAD-4 (Rohm & Haas, Frankfurt, Germany), and Serdolite PAD I, PAD II, and PAD III (Serva AG, Heidelberg, Germany). Furthermore, the adsorption onto the polymethacrylate/divinylbenzene Supelcogel TPR-100 (Supelco, Deisenhofen, Germany) was investigated. Characteristic parameters of the polymeric adsorbents (particle diameter, d_{Part}, specific surface, A_{BET}, pore diameter, d_P, and pore volume, V_P), as provided by the manufacturers, are listed in Table 2.

The phenolic substances to be adsorbed (see Table 3) were used without further purification. Their purities are listed in Table 4. Water was distilled and filtered four times (conductivity $\leq 1\ \mu S\ cm^{-1}$). It was degassed by ultrasonic treatment at reduced pressure before the measurements; an online vacuum degasser was used during the runs.

Experimental Procedure. The polystyrene bulk material was washed several times with methanol which had been dried with molecular sieves of 3 Å pore diameter (Fluka, Deisenhofen, Germany) and activated under vacuum at 513.15 K for 6 h. The methanol was replaced with water. The washing procedure ensured a complete wetting of the hydrophobic polymers. An HPLC glass column (Superformance 50-10, 10 mm i.d., 50 mm length; Götec, Darmstadt, Germany) was packed with the polymer slurry and equilibrated with water at a flow rate of 1.5 mL min^{-1} for 12 h. The polymethacrylate/divinylbenzene material was used in an industrially packed HPLC column (Supelcogel TPR-100, 4.6 mm i.d., 15 cm length) equilibrated with water. The weight of the dry adsorbent was determined after the

10.1021/je000283a CCC: $20.00
Published on Web 02/21/2001

Table 1. Adsorption Systems Examined in This Work

adsorption system			T/K
TPR-100	+ phenol	+ H_2O	296.15, 298.15, 307.15, 318.15
	+ 2-chlorophenol	+ H_2O	294.15, 307.15, 318.15
	+ 4-chlorophenol	+ H_2O	297.15, 308.15, 318.15
	+ 2,4-dichlorophenol	+ H_2O	295.15, 309.15, 318.15
	+ 2,6-dichlorophenol	+ H_2O	295.15, 308.15, 318.15
	+ 2,4,6-trichlorophenol	+ H_2O	298.15
	+ 1,2-dihydroxybenzene	+ H_2O	298.15, 308.15, 318.15
	+ 1,3-dihydroxybenzene	+ H_2O	298.15, 308.15, 318.15
Lewatit VP-OC 1163	+ phenol	+ H_2O	296.15
	+ 2-chlorophenol	+ H_2O	296.15
Amberlite XAD-4	+ phenol	+ H_2O	296.15
	+ 2-chlorophenol	+ H_2O	296.15
	+ 2,4-dichlorophenol	+ H_2O	296.15
Serdolite PAD I	+ phenol	+ H_2O	296.15
	+ 2,4-dichlorophenol	+ H_2O	296.15
Serdolite PAD II	+ phenol	+ H_2O	296.15
	+ 2-chlorophenol	+ H_2O	296.15
	+ 2,4-dichlorophenol	+ H_2O	296.15
Serdolite PAD III	+ phenol	+ H_2O	296.15
	+ 2-chlorophenol	+ H_2O	296.15
	+ 2,4-dichlorophenol	+ H_2O	296.15

Table 2. Characteristic Parameters of the Polymeric Adsorbents

polymer	d_{Part}/mm	A_{BET}/($m^2\ g^{-1}$)	d_P/nm	V_P/($cm^3\ g^{-1}$)
Supelcogel TPR-100	0.005	340	9.3	0.8
Lewatit VP-OC 1163	0.3−1.2	1400	0.5−10	0.8
Amberlite XAD-4	0.49−0.69	750	4	0.74
Serdolite PAD I	0.3−1.0	250	25	0.6
Serdolite PAD II	0.3−1.0	450	25	0.25
Serdolite PAD II	0.3−1.0	1000	20	0.3

Table 3. Physicochemical Properties of the Examined Phenols at 298.15 K

	M/(g mol^{-1})	$\tilde{c}^{sat}$/(g $L_{H_2O}^{-1}$)	pK_a
phenol (PHE)	94.11	80.23	9.95
2-chlorophenol (2CP)	128.56	21.02	8.44
4-chlorophenol (4CP)	128.56	18.32	9.29
2,4-dichlorophenol (24DCP)	163.00	5.03	7.77
2,6-dichlorophenol (26DCP)	163.00	2.65	6.79
2,4,6-trichlorophenol (246TCP)	197.45	0.42	6.19
1,2-dihydroxybenzene (catechin, CAT)	110.11	1121.51	
1,3-dihydroxybenzene (resorcin, RES)	110.11	1550.44	

Table 4. Purity of the Organic Substances

component	supplier	purity
phenol, for synthesis	Merck−Schuchardt	≥99%
2-chlorophenol	Lancaster	≥98%
4-chlorophenol	Sigma−Aldrich Chemie GmbH	≥99%
2,4-dichlorophenol	Sigma−Aldrich Chemie GmbH	≥99%
2,6-dichlorophenol	Sigma−Aldrich Chemie GmbH	≥99%
2,4,6-trichlorophenol	Sigma−Aldrich Chemie GmbH	≥98%
1,2-dihydroxybenzene	Sigma−Aldrich Chemie GmbH	≥99.5%
1,3-dihydroxybenzene	Sigma−Aldrich Chemie GmbH	≥99.9%
sodium hydroxide, aq	Sigma−Aldrich Chemie GmbH	0.0990 n
methanol, p.a.	E. Merck	≥99.8%

measurements with an analytic balance (Sartorius MCP210P, Göttingen, Germany, accuracy ±20 μg, reproducibility ±10 μg) by removing the polymer from the column and drying at 313.15 K under vacuum for 24 h. About 1 g of dry adsorbent was used. The polymer mass was determined to within $\pm 5 \times 10^{-4}$ g.

The surface excess for the adsorption of the phenols from aqueous solution onto the polymers was determined chromatographically by frontal analysis.[5] The composition of the solution of the phenols at the column inlet was changed in successive steps. A computer calculated the concentration at the column outlet from the signals of a UV spectrometer at 260 nm (Jasco 975-UV, Jasco Labor- und Datentechnik GmbH, Gross-Umstadt, Germany, and Shimadzu SPD 6AV, Shimadzu, Duisburg, Germany, respectively) by means of the corresponding calibration data measured previously. From the breakthrough curves for each concentration step, one point of the isotherm was derived by solving the integral mass balance equation. The concentration steps for the two HPLC columns were either formed by mixing of the phenolic stock solution and water on the high-pressure side of two HPLC pumps (Shimadzu LC-6A) or by actuating an eight-way switching valve (Hamilton MVP, HVXM 8-5, Hamilton Deutschland GmbH, Darmstadt, Germany) to select different sample fluid bottles. Gas washing bottles filled with a sealing liquid allowed a pressure adjustment in the sample fluid bottles and in the collecting tank without contaminating the surrounding atmosphere with phenolic vapors. Adsorption measurements at different temperatures were performed with the TPR-100 column using an HPLC column oven (Shimadzu CTO-6A) also used for thermostating the tubing of the incoming solution. The room temperature was maintained constant to within ±0.2 K.

Aqueous stock solutions of the phenolic adsorbates were prepared gravimetrically using an analytic balance (Sartorius MCP210P) for the sample and a Mettler PL3001 balance (accuracy ±0.1 g, reproducibility ±0.1 g) for water. Uncertainties for the determination of the mass of phenol, m_2, and that of water, m_3, amount to $\sigma_{m_2} = 1 \times 10^{-4}$ g and $\sigma_{m_3} = 0.1$ g, respectively. For the concentration of the phenolic solution as mass percentage of component 2, w_2, the error due to weighing inaccuracies can thus be determined to be $\pm 1.2 \times 10^{-4}$ mg g^{-1} according to the Gaussian law of error propagation (for $w_2 = 7 \times 10^{-4}$ and with an exemplary mass of the solution of 1000 g). For only slightly soluble phenols, the solution was heated to 323.15 K and stirred for up to 4 h in a closed vessel to ensure a homogeneous mixing.

The molar concentration of the stock solution, c_2, at the surrounding temperature, T_0, was calculated according to

$$c_2(T_0) = \frac{w_2}{M_2}\rho_{23}(T_0) \approx \frac{w_2}{M_2}\rho_3(T_0) \qquad (1)$$

with M_2 being the molar mass of the phenol. The concentration of the solution at the working temperature, T, of

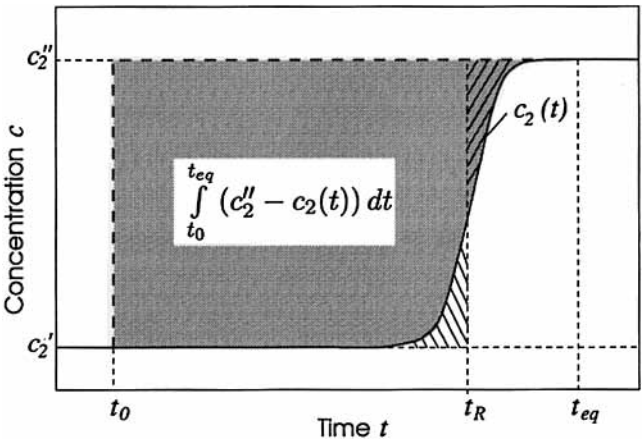

Figure 1. Determination of the retention time, t_R, with frontal analysis: – – –, concentration step; ———, breakthrough curve.

the column is given by

$$c_2(T) = c_2(T_0)\frac{\rho_3(T)}{\rho_3(T_0)} \tag{2}$$

The maximum concentration of the stock solutions was about 3.5 mmol L^{-1}. The error propagation law thus yields an uncertainty of $\sigma_{c_2} = 2 \times 10^{-3}$ mmol L^{-1} for the molar concentration of the phenolic solutions.

The phenol concentration for each adsorption step on the TPR-100 column was calculated from the flow rates of water, $\dot{V}_3$, and of the stock solution of the concentration $c_{2,\text{stock}}$, $\dot{V}_2$:

$$c_2(T_0) = c_{2,\text{stock}}(T_0)\frac{\dot{V}_2}{\dot{V}_2 + \dot{V}_3} \tag{3}$$

The void volume of the HPLC systems was determined by frontal analysis with an aqueous solution of sodium hydroxide (UV: 200 nm), which, according to information from the manufacturer and based on own laboratory experience, is not adsorbed onto the polymeric material. For the TPR-100 system, void volumes were determined for each concentration step in order to take into account the start-up and switching behavior of the pumps.

For a binary liquid mixture, the difference in the volume-based surface excess of the preferentially adsorbed component 2 (phenol), $\Delta n_2^{e(v)}$, related to the applied concentration step, $\Delta c_2 = c'' - c'$, is given by

$$\Delta n_2^{e(v)} = \int_{t_0}^{t_{eq}} (\dot{V}_{in} c_2'' - \dot{V}_{out} c_2(t))\,dt - \Delta c_2 V_{void} = \Delta c_2 (t_R \dot{V} - V_{void}) \tag{4}$$

with $\dot{V}_{in} \approx \dot{V}_{out} \approx \dot{V}$ = constant. The retention time of component 2, t_R, is determined by integrating the breakthrough curve; see Figure 1:

$$t_R = \frac{1}{\Delta c_2}\int_{t_0}^{t_{eq}} (c_2(t_{eq}) - c_2(t))\,dt \tag{5}$$

The adsorbed amount of component 2 is proportional to the shaded area in Figure 1.

The void volume of the HPLC systems, V_{void}, and the retention volume for the actual adsorption measurement, $V_R = t_R\dot{V}$, were determined in the same way. Due to the term $(t_R\dot{V} - V_{void})$ in eq 4, systematic errors for the determination of V_{void} and V_R are canceled out. Reproduction measurements yielded a mean uncertainty of 0.05 mL for the void volume. Since the flow rates for the adsorption measurements and for the determination of the void volume are the same, the same value can be attributed to the uncertainty of the retention volume, V_R. The uncertainty of the difference $\Delta V = t_R\dot{V} - V_{void}$ thus amounts to $\sigma_{\Delta V} = 0.1$ mL. The flow rate, $\dot{V}$, was determined for each concentration step by means of the mass of the collected liquid, the elapsed time, and the density of the fluid at the surrounding temperature. The error of the flow rate for a typical concentration step ($\dot{V} = 0.7$ mL min^{-1}) according to the error propagation law amounts to 1.6×10^{-4} mL min^{-1}. The calibration data for the determination of the phenol concentration from the UV-spectroscopic data are fitted with a mean uncertainty of 8×10^{-3} mmol L^{-1}. Taking into account the error resulting from the preparation of the phenolic solutions, σ_{c_2}, and a reproducibility of ±0.001 AU for the spectroscopic data, the uncertainty of the phenol concentration determined by means of the UV-detectors equals ±0.011 mmol L^{-1}. The maximum error for the concentration difference in eqs 4 and 5 can thus be given as $\sigma_{\Delta c_2} = 0.022$ mmol L^{-1}.

To determine the adsorption isotherm from the recorded breakthrough curves, the surface excess calculated according to eq 4 is divided by the mass of the adsorbent, m_A. The total mass-related surface excess, $\Gamma_2^{e(v)}$, for a concentration c_2 is given by the sum of the surface excesses for each concentration step i, $\Gamma_{2,i}^{e(v)}$, up to that concentration:

$$\Gamma_2^{e(v)} = \sum_{i=1}\Gamma_{2,i}^{e(v)} = \sum_{i=1}\frac{\Delta c_{2,i}}{m_A}(\dot{V}_i t_{R,i} - V_{void}) \tag{6}$$

The error of the surface excess, $\Gamma_2^{e(v)}$, cannot be determined with the Gaussian error propagation law, since the quantities of eqs 4 or 6, respectively, cannot be determined independently. Summing up the surface excesses for different concentration steps according to eq 6 results in a propagation of the uncertainties for each step. A faulty surface excess, $\Gamma_{2,i}^{e(v)}$, thus changes the position of the following isotherm points but does not influence the slope of the isotherm. Reproduction measurements for an entire isotherm (multiple adsorption and desorption measurements) and a comparison of the surface excess, $\Gamma_2^{e(v)}$, resulting from the summation of several concentration steps with the surface excess determined for one single concentration step and the same concentration yield a maximum error for the surface excess of the order of 2%. In a worst case estimation, the maximum relative error of the surface excess was determined to be 2.2% with the predominant factor being the uncertainty of the concentration difference.

Results and Discussion

Phenols are adsorbed physically onto the polymer surface by nonspecific van der Waals forces and specific interactive forces (dipole−dipole interactions, hydrogen bridge linkages). The adsorption is based on interactive forces between adsorbate and adsorbent, adsorbate and solvent, and solvent and adsorbent, respectively. The measured surface excess data for the adsorption systems polymer (1) + phenol (2) + water (3) at various temperatures are listed in Table 5.

Influence of the Adsorbate. Figure 2 shows adsorption isotherms for different phenols onto TPR-100 at temperatures between 294.15 and 298.15 K. Redlich−Peterson

Table 5. Adsorption Equilibria for Polymer (1) + Phenol (2) + Water (3)

c_2/mmol $L_{H_2O}^{-1}$	$\Gamma_2^{e(v)}$/mmol g^{-1}	c_2/mmol $L_{H_2O}^{-1}$	$\Gamma_2^{e(v)}$/mmol g^{-1}	c_2/mmol $L_{H_2O}^{-1}$	$\Gamma_2^{e(v)}$/mmol g^{-1}
TPR-100 (1) + Phenol (2) + Water (3), $T = 296.15$ K, $\tilde{c}_2^{sat} = 0.833$ mol $L_{H_2O}^{-1}$					
0.20	0.0109	1.46	0.0681	2.34	0.1035
0.41	0.0206	1.46	0.0672	2.59	0.1105
0.66	0.0320	1.49	0.0680	2.88	0.1207
0.71	0.0348	1.50	0.0711	2.93	0.1228
0.91	0.0439	1.78	0.0785	3.22	0.1360
0.99	0.0457	2.02	0.0853		
1.22	0.0570	2.21	0.0950		
TPR-100 (1) + Phenol (2) + Water (3), $T = 298.15$ K, $\tilde{c}_2^{sat} = 0.853$ mol $L_{H_2O}^{-1}$					
0.27	0.0138	1.05	0.0470	3.08	0.1157
0.27	0.0136	1.59	0.0678	3.52	0.1283
0.52	0.0250	2.08	0.0846		
0.54	0.0251	2.59	0.1005		
TPR-100 (1) + Phenol (2) + Water (3), $T = 306.15$ K, $\tilde{c}_2^{sat} = 0.942$ mol $L_{H_2O}^{-1}$					
0.25	0.0111	1.50	0.0557	2.95	0.0999
0.49	0.0204	1.74	0.0648	3.39	0.1119
0.74	0.0298	1.98	0.0711		
1.00	0.0390	2.46	0.0857		
TPR-100 (1) + Phenol (2) + Water (3), $T = 318.15$ K, $\tilde{c}_2^{sat} = 1.109$ mol $L_{H_2O}^{-1}$					
0.23	0.0073	1.02	0.0299	2.48	0.0702
0.27	0.0087	1.11	0.0330	2.75	0.0769
0.45	0.0141	1.11	0.0335	3.03	0.0836
0.52	0.0158	1.34	0.0397	3.30	0.0902
0.55	0.0169	1.56	0.0463	3.57	0.0965
0.67	0.0207	1.66	0.0490	3.83	0.1024
0.78	0.0247	1.94	0.0563	3.83	0.1029
0.89	0.0272	2.21	0.0634		
TPR-100 (1) + 2-Chlorophenol (2) + Water (3), $T = 294.15$ K, $\tilde{c}_2^{sat} = 0.150$ mol $L_{H_2O}^{-1}$					
0.34	0.0743	1.62	0.2423	3.20	0.3837
0.56	0.1092	1.88	0.2737	3.70	0.4203
0.84	0.1531	2.15	0.2945		
1.09	0.1829	2.67	0.3405		
TPR-100 (1) + 2-Chlorophenol (2) + Water (3), $T = 307.15$ K, $\tilde{c}_2^{sat} = 0.194$ mol $L_{H_2O}^{-1}$					
0.54	0.0846	2.08	0.2442	3.59	0.3585
1.05	0.1457	2.59	0.2857		
1.57	0.1982	3.10	0.3239		
TPR-100 (1) + 2-Chlorophenol (2) + Water (3), $T = 318.15$ K, $\tilde{c}_2^{sat} = 0.231$ mol $L_{H_2O}^{-1}$					
0.55	0.0691	1.87	0.1895	3.18	0.2924
1.08	0.1216	2.13	0.2101	3.69	0.3234
1.60	0.1678	2.66	0.2570		
TPR-100 (1) + 4-Chlorophenol (2) + Water (3), $T = 297.15$ K, $\tilde{c}_2^{sat} = 0.139$ mol $L_{H_2O}^{-1}$					
0.24	0.0676	1.24	0.2294	2.59	0.3595
0.52	0.1214	1.56	0.2610	2.87	0.3894
1.04	0.2009	2.07	0.3140	3.33	0.4275
TPR-100 (1) + 4-Chlorophenol (2) + Eater (3), $T = 308.15$ K, $\tilde{c}_2^{sat} = 0.181$ mol $L_{H_2O}^{-1}$					
0.23	0.0519	1.49	0.2172	3.42	0.3739
0.50	0.0958	1.98	0.2636		
1.00	0.1636	2.70	0.3224		
TPR-100 (1) + 4-Chlorophenol (2) + Water (3), $T = 318.15$ K, $\tilde{c}_2^{sat} = 0.219$ mol $L_{H_2O}^{-1}$					
0.25	0.0423	0.99	0.1335	2.46	0.2593
0.26	0.0426	1.48	0.1806	2.95	0.2933
0.50	0.0765	1.97	0.2223	3.44	0.3245
TPR-100 (1) + 2,4-Dichlorophenol (2) + Water (3), $T = 295.15$ K, $\tilde{c}_2^{sat} = 0.028$ mol $L_{H_2O}^{-1}$					
0.25	0.2275	1.48	0.6773	2.96	0.9512
0.50	0.3567	1.97	0.7811	3.66	1.0550
1.02	0.5479	2.44	0.8694		
TPR-100 (1) + 2,4-Dichlorophenol (2) + Water (3), $T = 309.15$ K, $\tilde{c}_2^{sat} = 0.040$ mol $L_{H_2O}^{-1}$					
0.24	0.1659	1.53	0.5641	3.05	0.8322
0.51	0.2815	2.03	0.6655	3.50	0.8954
1.01	0.4413	2.54	0.7545		
TPR-100 (1) + 2,4-Dichlorophenol (2) + Water (3), $T = 318.15$ K, $\tilde{c}_2^{sat} = 0.047$ mol $L_{H_2O}^{-1}$					
0.29	0.1674	1.16	0.4338	2.30	0.6537
0.59	0.2804	1.73	0.5539	2.86	0.7385
TPR-100 (1) + 2,6-Dichlorophenol (2) + Water (3), $T = 295.15$ K, $\tilde{c}_2^{sat} = 0.016$ mol $L_{H_2O}^{-1}$					
0.26	0.1519	1.51	0.5228	2.95	0.7828
0.53	0.2573	1.99	0.6190	3.45	0.8568
1.02	0.4055	2.46	0.7043		

Table 5 (Continued)

c_2/mmol $L_{H_2O}^{-1}$	$\Gamma_2^{e(v)}$/mmol g^{-1}	c_2/mmol $L_{H_2O}^{-1}$	$\Gamma_2^{e(v)}$/mmol g^{-1}	c_2/mmol $L_{H_2O}^{-1}$	$\Gamma_2^{e(v)}$/mmol g^{-1}
TPR-100 (1) + 2,6-Dichlorophenol (2) + Water (3), T = 308.15 K, $\tilde{c}_2^{sat}$ = 0.019 mol $L_{H_2O}^{-1}$					
0.23	0.1223	1.50	0.4827	2.93	0.7536
0.50	0.2229	1.98	0.5823	3.41	0.8241
1.01	0.3664	2.45	0.6700		
TPR-100 (1) + 2,6-Dichlorophenol (2) + Water (3), T = 318.15 K, $\tilde{c}_2^{sat}$ = 0.020 mol $L_{H_2O}^{-1}$					
0.26	0.1100	1.55	0.4320	3.00	0.6835
0.53	0.1919	2.03	0.5246	3.46	0.7509
1.05	0.3258	2.51	0.6073		
TPR-100 (1) + 2,4,6-Trichlorophenol (2) + Water (3), T = 298.15 K, $\tilde{c}_2^{sat}$ = 0.002 mol $L_{H_2O}^{-1}$					
0.16	0.4110	0.81	1.2300	1.90	1.6912
0.32	0.7238	1.13	1.3628		
0.56	1.0218	1.42	1.5136		
TPR-100 (1) + 1,2-Dihydroxybenzene (2) + Water (3), T = 298.15 K, $\tilde{c}_2^{sat}$ = 10.185 mol $L_{H_2O}^{-1}$					
0.27	0.0059	1.52	0.0273	3.03	0.0514
0.51	0.0100	2.02	0.0353	3.49	0.0579
1.01	0.0187	2.52	0.0431		
TPR-100 (1) + 1,2-Dihydroxybenzene (2) + Water (3), T = 308.15 K, $\tilde{c}_2^{sat}$ = 13.639 mol $L_{H_2O}^{-1}$					
0.25	0.0041	1.51	0.0226	2.94	0.0421
0.51	0.0083	2.01	0.0300	3.37	0.0476
1.01	0.0158	2.47	0.0359		
TPR-100 (1) + 1,2-Dihydroxybenzene (2) + Water (3), T = 318.15 K, $\tilde{c}_2^{sat}$ = 17.092 mol $L_{H_2O}^{-1}$					
0.27	0.0029	1.53	0.0178	3.03	0.0353
0.52	0.0059	2.03	0.0237	3.51	0.0406
1.01	0.0118	2.53	0.0295		
TPR-100 (1) + 1,3-Dihydroxybenzene (2) + Water (3), T = 298.15 K, $\tilde{c}_2^{sat}$ = 14.081 mol $L_{H_2O}^{-1}$					
0.26	0.0048	1.52	0.0226	3.00	0.0412
0.51	0.0089	2.02	0.0294	3.46	0.0468
1.01	0.0159	2.50	0.0347		
TPR-100 (1) + 1,3-Dihydroxybenzene (2) + Water (3), T = 308.15 K, $\tilde{c}_2^{sat}$ = 18.445 mol $L_{H_2O}^{-1}$					
0.26	0.0034	1.52	0.0191	3.01	0.0348
0.52	0.0074	2.03	0.0245	3.49	0.0401
1.02	0.0132	2.52	0.0301		
TPR-100 (1) + 1,3-Dihydroxybenzene (2) + Water (3), T = 318.15 K, $\tilde{c}_2^{sat}$ = 22.809 mol $L_{H_2O}^{-1}$					
0.26	0.0027	1.53	0.0140	2.99	0.0262
0.51	0.0048	2.02	0.0183	3.46	0.0300
1.02	0.0095	2.51	0.0223		
Lewatit VP-OC 1163 (1) + Phenol (2) + Water (3), T = 296.15 K, $\tilde{c}_2^{sat}$ = 0.833 mol $L_{H_2O}^{-1}$					
0.29	0.3176	2.11	1.1853	3.84	1.5702
0.33	0.3527	2.57	1.3108	3.91	1.5852
0.45	0.5179	2.97	1.4022	4.39	1.6250
0.87	0.7208	3.09	1.4271	4.87	1.6988
0.91	0.7612	3.31	1.5085	4.88	1.7506
1.44	0.9721	3.42	1.5468	5.85	1.8935
1.96	1.1126	3.82	1.5663		
Lewatit VP-OC 1163 (1) + 2-Chlorophenol (2) + Water (3), T = 296.15 K, $\tilde{c}_2^{sat}$ = 0.157 mol $L_{H_2O}^{-1}$					
0.23	0.8726	1.44	2.1492	3.05	2.8950
0.47	1.3353	1.94	2.4601	3.44	3.0677
0.95	1.7689	2.57	2.7728		
XAD-4 (1) + Phenol (2) + Water (3), T = 296.15 K, $\tilde{c}_2^{sat}$ = 0.833 mol $L_{H_2O}^{-1}$					
0.27	0.1400	1.54	0.4097	2.87	0.5772
0.51	0.2110	1.96	0.4689	3.51	0.6403
0.90	0.2992	2.40	0.5250		
XAD-4 (1) + 2-Chlorophenol (2) + Water (3), T = 296.15 K, $\tilde{c}_2^{sat}$ = 0.157 mol $L_{H_2O}^{-1}$					
0.30	0.4581	1.44	0.8948	2.82	1.1680
0.52	0.6054	1.89	0.9985	3.25	1.2352
0.97	0.7907	2.42	1.1017	3.50	1.2734
XAD-4 (1) + 2,4-Dichlorophenol (2) + Water (3), T = 296.15 K, $\tilde{c}_2^{sat}$ = 0.029 mol $L_{H_2O}^{-1}$					
0.50	1.2319	1.98	1.9252	3.56	2.3537
0.99	1.5275	2.49	2.0782		
1.49	1.7513	2.99	2.2184		
PAD I (1) + Phenol (2) + Water (3), T = 296.15 K, $\tilde{c}_2^{sat}$ = 0.833 mol $L_{H_2O}^{-1}$					
0.26	0.0442	1.49	0.1392	2.93	0.2040
0.49	0.0683	1.89	0.1602	3.45	0.2226
0.97	0.1069	2.48	0.1862		
PAD I (1) + 2,4-Dichlorophenol (2) + Water (3), T = 296.15 K, $\tilde{c}_2^{sat}$ = 0.029 mol $L_{H_2O}^{-1}$					
0.17	0.3693	1.44	0.7051	2.92	0.8901
0.44	0.4843	1.90	0.7739	3.50	0.9480
0.94	0.6181	2.42	0.8388		

Table 5 (Continued)

c_2/mmol $L^{-1}_{H_2O}$	$\Gamma_2^{e(v)}$/mmol g^{-1}	c_2/mmol $L^{-1}_{H_2O}$	$\Gamma_2^{e(v)}$/mmol g^{-1}	c_2/mmol $L^{-1}_{H_2O}$	$\Gamma_2^{e(v)}$/mmol g^{-1}
PAD II (1) + Phenol (2) + Water (3), T = 296.15 K, $\tilde{c}_2^{sat}$ = 0.833 mol $L^{-1}_{H_2O}$					
0.27	0.0518	1.50	0.1729	2.95	0.2590
0.50	0.0821	1.96	0.2001	3.37	0.2809
1.00	0.1329	2.46	0.2310		
PAD II (1) + 2-Chlorophenol (2) + Water (3), T = 296.15 K, $\tilde{c}_2^{sat}$ = 0.157 mol $L^{-1}_{H_2O}$					
0.29	0.2330	1.46	0.5325	2.44	0.6702
0.53	0.3274	2.00	0.6148	3.54	0.7373
1.06	0.4682	2.40	0.6646		
PAD II (1) + 2,4-Dichlorophenol (2) + Water (3), T = 296.15 K, $\tilde{c}_2^{sat}$ = 0.029 mol $L^{-1}_{H_2O}$					
0.31	0.5740	1.47	1.0121	2.94	1.2901
0.46	0.6577	1.95	1.1148	3.32	1.3462
0.95	0.8666	2.46	1.2153		
PAD III (1) + Phenol (2) + Water (3), T = 296.15 K, $\tilde{c}_2^{sat}$ = 0.833 mol $L^{-1}_{H_2O}$					
0.26	0.3427	1.57	0.9131	2.99	1.2212
0.50	0.4998	2.04	1.0377	3.46	1.2980
1.00	0.7203	2.50	1.1338		
PAD III (1) + 2-Chlorophenol (2) + Water (3), T = 296.15 K, $\tilde{c}_2^{sat}$ = 0.157 mol $L^{-1}_{H_2O}$					
0.26	0.8066	0.99	1.6233	1.97	2.1243
0.50	1.2070	1.50	1.9175	2.34	2.2592
PAD III (1) + 2,4-Dichlorophenol (2) + Water (3), T = 296.15 K, $\tilde{c}_2^{sat}$ = 0.029 mol $L^{-1}_{H_2O}$					
0.40	2.2187	1.50	3.3227	2.99	3.9065
0.70	2.6505	1.98	3.5249	3.46	4.0247
0.99	2.9437	2.50	3.7315		

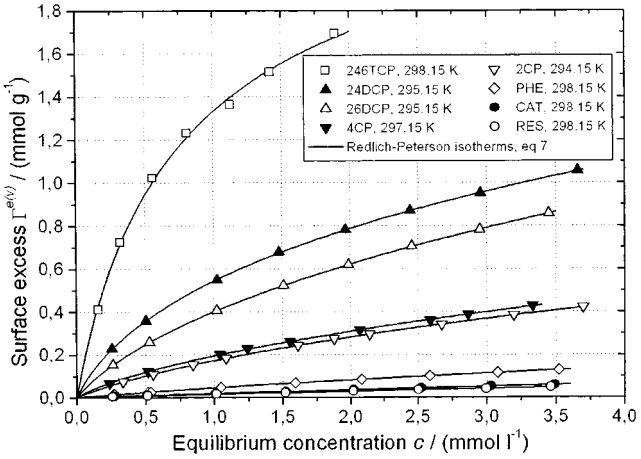

Figure 2. Adsorption isotherms for different phenols onto TPR-100.

isotherms[6] according to eq 7 are fitted to the experimental data.

$$\Gamma_2^{e(v)} = \frac{A_1 c_2}{1 + A_3 c_2^{A_2}} \qquad (7)$$

For energetically heterogeneous adsorbent surfaces, it holds that $A_2 \neq 1$. $A_2 = 1$ yields the Langmuir adsorption isotherm for homogeneous surfaces. For small concentrations, eq 7 is reduced to the Henry equation with A_1 corresponding to the Henry coefficient. For $A_2 = 1$, $\Gamma_2^{e(v)}$ approaches the saturation capacity for high concentrations, which is given by A_1/A_3. For the adsorption systems considered in this work (see Table 1), it holds that $A_2 < 1$. The heterogeneity of the adsorbent surfaces is confirmed by measurements of the isosteric adsorption enthalpy, which strongly varies with the surface excess, $\Gamma_2^{e(v)}$.

Interactive forces contributing to the adsorption process are mainly influenced by the following parameters: the electronegativity of the adsorptive (influence of the substituent), the hydrophobicity of the adsorptive, the intramolecular interactions, and the steric hindrance.

Due to the additional hydroxyl group on the aromatic ring, the adsorption capacity of TPR-100 for dihydroxybenzenes is reduced compared to that for phenol while it is increased for chloro-substituted phenols. Functional groups in the aromatic ring change its electron density. The aromatic ring of, for example, 2- or 4-chlorophenol is charged more negatively than the aromatic ring of a nonsubstituted phenol. The greater electron density in the ring supplies more π-electrons to interact with the adsorbent; the adsorptive interactions with the aromatic rings of the polymer are thus increased.

Moreover, steric effects play an important role for the adsorbability of the phenols. As shown in Figure 2, substitution of phenol with a chloro group in the ortho position results in a smaller adsorbability than substitution in the para position. 4-Chlorophenol is slightly better adsorbed than 2-chlorophenol, and 2,4-dichlorophenol is significantly more strongly adsorbed than 2,6-dichlorophenol. Due to the formation of multiple hydrogen bonds between the adsorbent and neighboring hydroxyl groups of the substituted phenols, 1,2-dihydroxybenzene is more strongly adsorbed than 1,3-dihydroxybenzene.

Phenolic substances have a limited solubility in water. The hydrophobic aromatic ring of the phenol associates with the equally hydrophobic polymer.[7] Unsubstituted phenol forms strong hydrogen bonds with water. For chlorinated phenols, the formation of such intermolecular hydrogen bonds is reduced either by the formation of intramolecular bonds between the hydroxyl group and the substituent or by steric hindrance causing a reduced solubility in water and, consequently, an increasing adsorbability. Solubilities for the phenols considered in this work are given in Tables 3 and 5, respectively.

Temperature Dependence of the Adsorption. In Figure 3, adsorption isotherms for TPR-100 + (phenol, 2-chlorophenol, or 1,3-dihydroxybenzene, respectively) + water are displayed as a function of temperature. The surface excess for the phenols, $\Gamma_2^{e(v)}$, is decreased significantly with increasing temperature due to the exothermic adsorption process. The reduction of the adsorbate/adsorbent interaction with increasing temperature is reinforced by the temperature dependence of the solubility of the

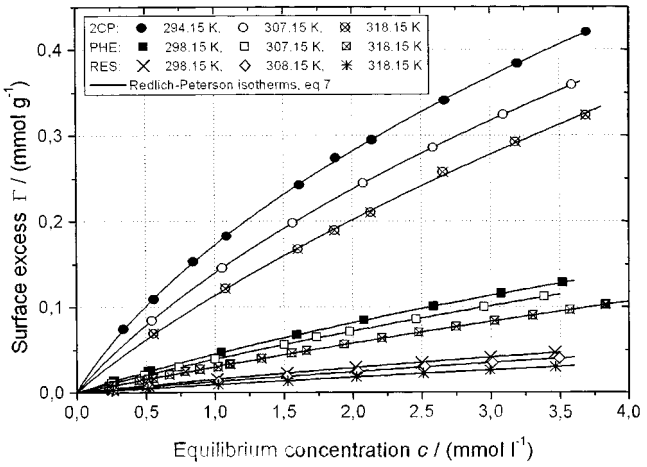

Figure 3. Temperature dependence of the adsorption of three phenols onto TPR-100.

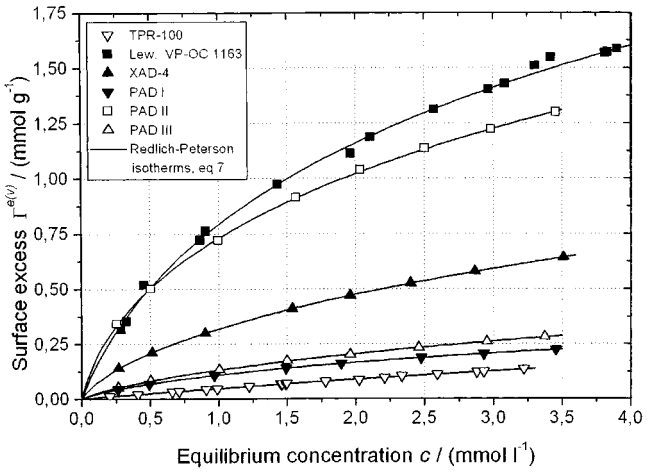

Figure 4. Adsorption isotherms for different polymers + phenol + water at 296.15 K.

phenols. The better the molecules are solvated at higher temperatures, the smaller their tendency to adsorb onto the polymer surface. The percental decrease of the hydrophobicity of the molecule to be adsorbed with increasing temperature corresponds to the percental increase in the surface excess. The temperature dependence of the adsorption of phenols from aqueous solution onto polymers is thus clearly dominated by the solubility effect.

Influence of the Adsorbent. Phenol, 2-chlorophenol, and 2,4-dichlorophenol were adsorbed onto different styrene or methacrylate polymers cross-linked with divinylbenzene (see Table 5). Figure 4 shows different adsorption isotherms for phenol at 296.15 K.

The adsorption capacity for phenol is greater for polystyrene than for polymethacrylate, which is attributed to the greater hydrophobicity of polystyrene, resulting in a better adsorption of the equally hydrophobic phenols. The adsorption capacity for phenol increases with an increasing BET surface of the polymer. Because of steric and/or diffusion effects, the increase is not linear. The surface excess increases with the degree of cross-linking of the polymers. Post-cross-linked polymers such as Lewatit VP-OC 1163 or PAD III thus show much larger adsorption capacities for phenol than polymers without chemical post-cross-linking, for example, XAD-4.[8] In the post-cross-linking process, the specific surface area of the polymers is increased; micropores are created while the amount of macropores remains basically constant. For small adsorbate concentrations, more phenol is adsorbed due to the micropore filling mechanism than could be expected due to a mere adsorption on the pore walls of non-cross-linked material.

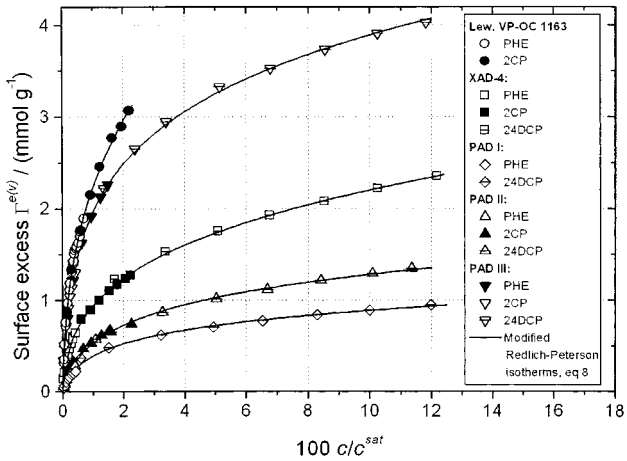

Figure 5. Characteristic adsorption isotherms for polystyrenes + phenols + water at 296.15 K.

Normalization of the Adsorption Isotherms. To model the adsorption of phenols onto polymeric adsorbents, the fluid phase concentration of phenol is normalized according to Traube's rule[9−11] by means of the solubility of the phenol to be adsorbed, c^{sat}. Adsorbate/water and adsorbate/polymer interactions can thus be taken into account separately. Modified Redlich−Peterson isotherms, so-called characteristic isotherms,

$$\Gamma_2^{e(v)} = \frac{\hat{A}_1(c_2/c_2^{sat})}{1 + \hat{A}_3(c_2/c_2^{sat})^{\hat{A}_2}} \qquad (8)$$

are used to fit the normalized adsorption data. Normalized adsorption isotherms for polystyrene adsorbents are shown in Figure 5; for the polymethacrylate TPR-100, they are displayed in Figure 6. Solubility data, that is, the saturation concentrations of the phenols in mol $L_{H_2O}^{-1}$, c_2^{sat}, are included in Table 5. Due to the normalization of the adsorption data, the parameters $\hat{A}_1$ to $\hat{A}_3$ of the modified Redlich−Peterson isotherm, eq 8, should be regarded as correlation coefficients only.

The eight phenols under consideration can be divided into three groups: (a) dihydroxybenzenes (1,2- and 1,3-dihydroxybenzene), (b) phenol and chloro-substituted phenols which do not have two chloro atoms in the ortho position (phenol, 2- and 4-chlorophenol, 2,4-dichlorophenol), and (c) higher substituted phenols with two chloro groups in the ortho position (2,6-dichlorophenol, 2,4,6-trichlorophenol).

The characteristic adsorption isotherms for TPR-100 represent not only adsorption data for different adsorbates but also data for different temperatures. Temperature-dependent adsorption equilibria are thus reduced to the temperature dependence of the solubility of the phenols. The plot of the surface excess versus the normalized fluid-phase concentration shows that a change in adsorbate/water interactions is the basic reason for the different adsorbabilities of the phenols from water. For a given normalized concentration, the adsorption is best for dihydroxybenzenes, which show a high tendency for building hydrogen bridges between the aromatic hydroxyl groups and the adsorbent. Chlorophenols with two chloro substituents in the ortho position are the least adsorbed due to intramolecular hydrogen bonds between the hydroxyl group

Table 6. Prediction of Adsorption Equilibria

	database			
polymer	correlation	prediction	$RMSD_{corr}$/%	$RMSD_{pred}$/%
TPR-100	PHE, 2CP, 4CP	24DCP	0.58 (98)	0.66 (22)
Lewatit VP-OC 1163	PHE	2CP	0.72 (20)	2.06 (8)
XAD-4	PHE, 24DCP	2CP	0.93 (15)	1.46 (9)
PAD I	PHE	24DCP	0.08 (8)	4.31 (8)
PAD II	PHE, 24DCP	2CP	2.09 (16)	4.46 (8)
PAD III	PHE, 24DCP	2CP	1.92 (16)	0.94 (8)

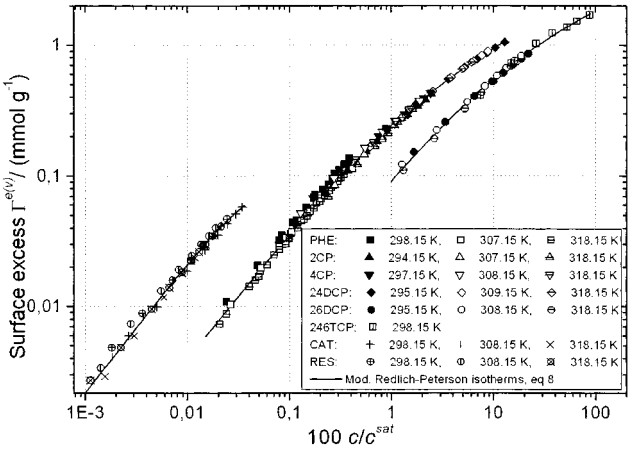

Figure 6. Characteristic adsorption isotherms for TPR-100 + phenols + water.

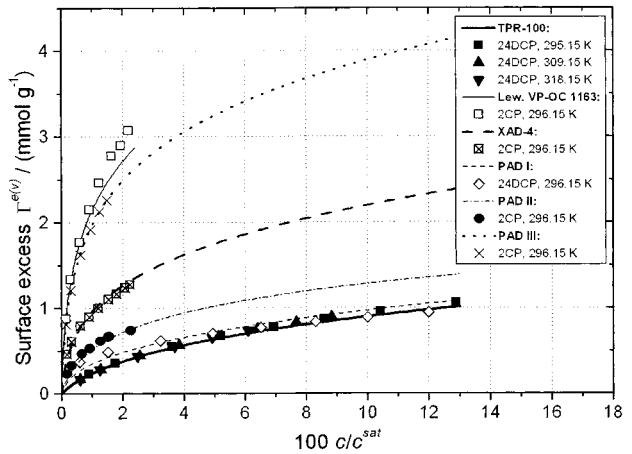

Figure 7. Comparison of adsorption equilibria predicted with characteristic isotherms (lines) and measured data (symbols).

and the chloro groups in the ortho position and the corresponding reduced formation of adsorbate/polymer bonds. Furthermore, hydrogen bonds between the functional groups of the phenols and the polymer are sterically hindered.

Using characteristic isotherms according to eq 8, adsorption equilibria for different adsorbates onto the same polymer can be described with only one set of parameters. For a prediction of adsorption equilibria with characteristic isotherms, the adsorption database was split into data used for the correlation and data used to verify the predicted adsorption equilibria. Figure 7 shows a prediction of adsorption equilibria for different polymers for adsorbates of group b. Characteristic adsorption isotherms resulting from the correlation of the reduced database are represented by lines. The symbols refer to measured data which were not used for the correlation. In Table 6, the correlation and prediction uncertainties for each characteristic isotherm, $RMSD_{corr}$ and $RMSD_{pred}$, respectively, and, in parentheses, the corresponding number of data points are given. The root of the mean square deviation, RMSD, is calculated according to

$$\mathrm{RMSD} = \frac{1}{N}\sqrt{\sum_i \left(\frac{\Gamma_i^{e(v)} - \Gamma_i^{e(v),\mathrm{calc}}}{\Gamma_i^{e(v)}}\right)^2} \qquad (9)$$

Prediction and correlation uncertainties are of the same order of magnitude. If the correlation database is large enough and covers the concentration range for which adsorption data are to be predicted, prediction uncertainties are in the range of 2%. The uncertainty of the surface excess for a prediction of adsorption data ($\Gamma_2^{e(v)}$, c_2) is identical to the uncertainty for a prediction of adsorption data with normalized concentration ($\Gamma_2^{e(v)}$, c_2/c_2^{sat}). The shape of the isotherm is predicted correctly even if the correlation data do not cover the whole range of the normalized concentration for which adsorption data are predicted, for example, for TPR-100. Adsorption data for $0 \le c_2/c_2^{sat} \le 2.5\%$ were used for the correlation while data were predicted up to $c_2/c_2^{sat} \approx 13\%$. Nevertheless, the uncertainty for the prediction does not exceed the correlation uncertainty significantly ($RMSD_{corr}$ = 0.58%, $RMSD_{pred}$ = 0.66 %).

The parameters $\hat{A}_1$ to $\hat{A}_3$ for the characteristic isotherms for each polymer, correlated to the entire database, are listed in Table 7 together with the standard deviation of the data fit, σ, and the root of the mean square deviation, RMSD, according to eq 9. The lettering refers to the adsorbate groups listed above. For the polystyrenes, only data at 296.15 K were used for the correlation so that, strictly speaking, a prediction of adsorption equilibria is limited to this temperature, as well. However, on the basis of the results for TPR-100, for which the temperature dependence of the adsorption equilibria is entirely taken

Table 7. Parameters and Correlation Deviations for Characteristic Adsorption Isotherms

polymer	$\hat{A}_1$/(mmol g^{-1})	$\hat{A}_2$	$\hat{A}_3$	σ/(mmol g^{-1})	RMSD/%
TPR-100 (a)	2.3330	1.0000	10.6315	0.0013	1.03
TPR-100 (b)	0.4095	0.6616	0.7307	0.0057	0.47
TPR-100 (c)	0.1088	0.7061	0.1930	0.0268	0.77
Lewatit VP-OC 1163 (b)	18.3566	0.6556	7.2485	0.0303	0.68
XAD-4 (b)	6.7178	0.6828	6.1298	0.0215	0.53
PAD I (b)	1.2982	0.7707	2.3090	0.0274	2.18
PAD II (b)	1.6136	0.7578	2.0262	0.0250	1.72
PAD III (b)	10.4646	0.7759	4.3368	0.0400	1.47

into account by the solubility of the phenols, it can be assumed that the given parameter sets for the polystyrenes can also be used to predict adsorption equilibria at temperatures other than 296.15 K.

Conclusion

For a reliable design of fluid-phase adsorption processes and a broader use of polymeric adsorbents, data on adsorption equilibria must be available. Thus, in this work, equilibrium data for the adsorption of phenols from aqueous solution onto different polymers are presented. The surface excess was determined using the chromatographic method of frontal analysis. The adsorption of eight phenols (phenol, chlorophenols, dihydroxybenzenes) onto six polymers (polystyrenes or polymethacrylate cross-linked with divinylbenzene) has been investigated for temperatures between 294.15 K and 318.15 K.

Characteristic adsorption isotherms of the Redlich−Peterson type permit the prediction of adsorption equilibria for different adsorbates with an uncertainty of 2%. The fluid-phase concentration is normalized to the solubility of the adsorbate in water to consider adsorbate/solvent interactions. A plot of the surface excess versus the normalized fluid-phase concentration yields three groups of characteristic isotherms for each polymer (dihydroxybenzenes, substituted phenols with two chloro atoms in the ortho position, and phenol and other substituted phenols). Parameters for the characteristic isotherms and solubilities for different phenols in water are given.

Literature Cited

(1) Elvers, B., Hawkins, S., Schulz, G., Eds. *Ullmanns Encyclopedia of Industrial Chemistry*, 5th ed.; VCH Verlagsgesellschaft mbH: Weinheim, 1991; Vol. A19.

(2) Rippen, G. *Umweltchemikalien*; Ecobase Media Explorer, ecomed Verlagsgesellschaft AG & Co. KG, 1998.

(3) Weissermel, K.; Arpe, H.-J. *Industrielle organische Chemie: bedeutende Vor- und Zwischenprodukte*, 5th ed.; Wiley-VCH Verlag GmbH: Weinheim, 1998.

(4) Exon, J. H. A Review of Chlorinated Phenols. *Vet. Hum. Toxicol.* **1984**, *26* (6), 508−520.

(5) Köster, F.; Findenegg, G. H. Adsorption from Binary Solvent Mixtures onto Silica Gel by HPLC Frontal Analysis. *Chromatographia* **1982**, *15* (12), 743−747.

(6) Redlich, O.; Peterson, D. L. A Useful Adsorption Isotherm. *J. Phys. Chem.* **1959**, *63*, 1024.

(7) Ferraro, J. F. Polymeric Adsorbers. *Technol. Mitt.* **1987**, *6*, 334−338.

(8) Kowalzik, A.; Wahl, A.; Pilchowski, K. Comparison of Traditional and New Adsorber Polymers for the Adsorption of 1,2-Dichloroethan from Water. *Acta Hydrochim. Hydrobiol.* **1996**, *24*, (1), 36−38.

(9) Urano, K.; Koichi, Y.; Yamamoto, E. Equilibria for Adsorption of Organic Compounds on Activated Carbons in Aqueous Solution. *J. Colloid Interface Sci.* **1982**, *86*, (1), 43−50.

(10) Radeke, K.-H.; Hartmann, G. On the Temperature Dependence of Adsorption of Organic Materials from Aqueous Solution. *Adsorption Sci. Technol.* **1992**, *8* (3), 153−157.

(11) Kim, H.-J.; Lee, S.-S.; Sohn, J.-E.; Furuya, E.; Takeuchi, Y.; Noll, K. E.; Yamashita, S. Adsorption of Phenols onto Macroreticular Resin Particles. *Korean J. Chem. Eng.* **1996**, *13* (4), 399−403.

Received for review August 25, 2000. Accepted November 22, 2000.

JE000283A